White Paper Presented at the 2024 Pipeline Pigging and Integrity Management Exhibition.

Advanced Technology for Tensile and Fracture Toughness Characterization of In-Service Piping

Michael P. Manahan, Sr.[1]
[1]MP Machinery and Testing, LLC

Pipeline Pigging and Integrity Management Exhibition

February 12-16, 2024

[1] Founder/Executive Chairman
MP Machinery and Testing, LLC
2161 Sandy Drive
State College, PA 16803
814-234-8860 (ext. 121)

Abstract

MPM developed the Instrumented Indentation System (I2S) for measurement of yield stress (YS), ultimate tensile strength (UTS), hardness, and ductility of in-service pipes. The I2S non-destructively indents the pipe surface while measuring applied load/deflection to determine the Brinell hardness. The pipe surface preparation is completed in less than 5 minutes and multiple data points for base, weld, and heat-affected-zones can be acquired in a few minutes. The I2S material model software displays the YS, UTS, and ductility on the portable computer immediately after measurement. The efficacy of the I2S data has been demonstrated by comparison with benchmark laboratory data obtained in the Pipeline Research Council International (PRCI) study and also with the Gas Technology Institute (GTI) benchmark data.

Not all pipes will pass the I2S screening. Therefore, for pipes that require plane-strain fracture toughness data, MPM has developed a miniaturized Charpy V-notch (MCVN) impact test that provides Charpy and fracture toughness data from a dynamic test measurement. It will be necessary to trepan small pieces of material (~0.2 inch x~ 0.2 inch x ~1.0 inch long) from the pipe and perform a weld repair as needed. MPM's test machine is equipped with an instrumented striker for acquisition of the dynamic load and deflection. The advanced mechanics model uses the load/deflection data to determine the material J-resistance (JR) curve and the fracture toughness (J_{IC} and K_{IC}). While it is recognized that other researchers have proposed correlations between Charpy energy (or tensile data) and plane-strain fracture toughness, MPM's experience shows that these correlations are only valid over limited materials and conditions. The robust approach is, therefore, to make a direct measurement of the fracture toughness.

Introduction.

Catastrophic fracture of gas transmission pipelines has led to the formulation of federally mandated inspection requirements for buried pipe in cases where the material properties are unknown. The so-called "Mega Rule" by the Pipeline and Hazardous Materials Safety Administration (PHMSA), is perhaps the most far-reaching rulemaking in decades. An important aspect is the requirement to measure mechanical properties on in-service piping. MPM developed the I2S for this purpose and the I2S measurements can be made without the need to shut down the transmission of the product. The I2S provides base and weld metal YS, UTS, hardness, and ductility using a shallow indentation at the surface of the pipe. If the properties meet the expected minimums, no further work is needed.

It is clear that not all pipes will have acceptable properties, and additional testing may be needed. MPM has developed a miniaturized Charpy test, that can be tested statically or dynamically, to produce a load-deflection curve that can be analyzed to determine the J-resistance curve and plane-strain fracture toughness of the material. These material data can then be used to compare with finite element calculated applied J levels for postulated flaws in the pipe. If the applied J is less than the measured J_{IC} with sufficient margin, then the pipe will not experience propagation of the postulated crack. This technology is described below, along with the I2S method for measurement of tensile properties. Together, these technologies offer powerful tools for assessing pipeline safety.

I2S method.

Since the inception of spherical indentation testing by Brinell and Meyers over 100 years ago, indentation techniques have become the standard method for measuring the hardness of materials. Over the past few decades, instrumentation of the indentation test has provided the opportunity to obtain more accurate and repeatable indentation data. Instrumented indentation involves the use of both a calibrated load cell and a displacement transducer. During the instrumented test, both the load and deflection are acquired during loading and unloading. Loads can be applied under either load or displacement control. This advanced measurement technique differs from the standard Brinell testing wherein a load is applied, held for a short duration, and then the diameter of the indentation is determined using a laboratory measuring microscope. The I2S determines the diameter from the load and deflection data, making the use of a measuring microscope optional. MPM also uses a high precision portable lens system for measuring the indentation diameter on the pipe under investigation. The I2S, when applied to piping characterization, consists of two key parts: the high precision field equipment used to precisely measure load/deflection on a buried pipe; and the material model to determine YS, UTS, and ductility. Each are discussed below and the benchmark data are presented to show the efficacy of the I2S results.

Equipment for buried pipe measurement.

Figure 1 shows the MPM I2S installed on a 16 inch diameter pipe. High force rotatable magnets are used to hold the indenter on the curved pipe until the chain come-along is attached around the pipe. The indenter can also be installed on a non-magnetic pipe in which case only the chain come-along is used. The chain come-along is connected to the

indenter handles to ensure there is no movement of the I2S during loading. The I2S can be configured with or without a battery power supply. An example system configuration with a battery power supply and hand truck is shown in Figure 1. The I2S-Field Application (I2S-FA) system has also been designed to operate from a pickup truck, or it can be transported to a pipe inspection location using an all-terrain vehicle (ATV) for cases where it is not possible to drive a motor vehicle. If truck access is possible, the power supply can be left on the truck in a secured position. If not, the I2S, power supply cart, and control computer can be carried to the inspection location manually.

There is no theoretical basis for stress-strain from the indentation test.

During the early 1900 time period, there was general agreement that hardness tests were very useful for practical industrial applications, but there was no consensus regarding the property of the material that was being measured in the indentation test. While empirical correlations were reported in the literature, there was mention in the early literature of the potential for a comprehensive theoretical basis for the correlations. Reference [1] presents a brief review of the early thinking regarding hardness data interpretation leading up to the work of Tabor. This reference points to Meyer's and Brinell's understanding that the ball indentation process did result in localized work hardening. Brinell had discovered an empirical relation that UTS is proportional to Brinell hardness (HBW):

$$UTS = a\,(HBW), \tag{1}$$

where "a" is an empirical constant ranging from 0.34 to 0.36 for steels with a wide range of carbon contents. Further, Meyer had deduced from ball indentation experiments that the applied load (W) is proportional to the chordal diameter (d) raised to a power "m":

$$W = k\,d^m \tag{2}$$

This exponent is referred to as the Meyer index.

Hutchings credits Tabor's work [2] as having provided the scientific basis for the hardness test. Hutchings states [1]:

> "The scientific basis for the indentation test had been only poorly appreciated when Tabor published his ground-breaking 'simple theory' in 1948: a model based on recent theoretical developments, careful experiments, and not a little inspiration, which provided the physical insight to drive the subject forward, and formed the basis of his own work and that of his collaborators, for the next 30 years. His book on hardness remains the most highly cited text on the subject by a large margin, more than 50 years after publication. All those working in the field of indentation science owe him a great debt."

There is no question that Tabor's work is the most widely reviewed hardness literature of all time. However, as will be discussed further below, research at MPM has demonstrated that while Tabor's equations, and those of follow-on researchers, work for a specific collection of materials, they are not applicable to a broad range of metals or ferrous alloys. Before discussing this point further, a brief summary of the concepts that Tabor had drawn together from the literature available to him at the time of his work is presented along with Tabor's supposed "theoretical" work.

When a spherical indenter is used to test a material, the indentation which remains after the load is removed has a larger radius of curvature than the indenter itself. What was lacking in the early days of indentation testing was a theoretical treatment of this phenomenon.

Tabor is appropriately credited with showing that the Hertz model for the elastic contact deformation of spherical bodies could predict the effect accurately. In addition, Tabor accurately described in qualitative terms how indentation by a ball led to elastic deformation, then to plastic flow with associated work hardening, and finally to elastic recovery after removal of the load. Tabor also applied developments in continuum mechanics by Timoshenko and others to the plastic deformation stage of indentation. As part of this work, Tabor noted that his data, and the data of other researchers, predicted a value of approximately 3 for the constraint factor, C, in the following relation:

$$P_m = C\ (YS) \tag{3}$$

In this equation, P_m is the mean contact pressure. This equation is purely empirical. Comparing equations (1) and (3) for a material with low work hardening, Tabor suggested a theoretical basis that supported the purely empirical equation (1). Tabor said that that geometrically similar indentations would induce similar strain distributions. He defined a 'representative strain' as being proportional to d/D, where D represents the diameter of the indenter. Tabor used the experimental data published earlier by Krupkowski for indentations with various ball diameters to show that geometrically similar indentations in a work-hardening metal showed identical values of P_m [3].

Next, Tabor went on to assert that for work-hardening metals, a plot of the mean indentation pressure versus d/D closely reproduced the true stress-strain curve. In his analysis, Tabor added the requirement that the pressure and uniaxial stress must be related by equation (3) with C= 2.8. Further, he defined the 'representative strain' as 0.2 d/D (arbitrary definition to match data). Tabor went on to assert that, for a metal that exhibited power-law hardening,

$$\sigma = \varepsilon^n. \tag{4}$$

Meyer's laws could be derived from the assumption that the strain was proportional to d/D. In this case, Tabor suggested that the Meyer index m would then be equal to the strain hardening exponent plus 2 (i.e., 2 + n). There is no physical basis for this assumption. Finally, Tabor analyzed geometrically similar indentations formed by the pyramidal Vickers indenter and showed experimentally that the 'representative strain' is approximately 8%. Hutchings concluded,

> "Thus, Tabor built up a theoretical model for the indentation of metals, validated by his experiments and the experiments of others, which in principle could explain the correlation between hardness and tensile strength, the variation of hardness seen in strain-hardening materials and expressed empirically by Meyer's laws, and the differences between the hardness values measured with indenters of different geometries. It provided a direct and quantitative link between the hardness test and the tensile or compressive stress-strain curve."

MPM research on the Tabor work has clearly indicated that his approach to correlation of indentation hardness with YS and UTS only works, at best, on a limited group of materials. In the above discussion, it was pointed out that the Tabor "theoretical" work, as described by Hutchings in Reference [1], is actually correlation work. Rather than go through all of the details of Tabor's work, it is expedient to focus on the basis for the YS and UTS models that are widely used today. Various researchers, including Tabor, have proposed different correlations, but all of these equations have the following form:

$$UTS = H\ (f(n)) \tag{5}$$

where, H is a measure of hardness and f(n) is a function of the power law hardening exponent n. A similar relation has been proposed by other researchers for the YS determination from

a hardness measurement. Of course, the key question here is how to obtain n, given the fact that it is the tensile property we seek to obtain from the hardness measurement. Tabor obtained the Meyer coefficient (m) from a log-log plot of the indentation load versus the indentation diameter. The strain hardening exponent was defined as:

$$n = m - 2 \tag{6}$$

The results obtained using Tabor's equations (5) and (6) work reasonably well for some materials, but yield very bad results for others. Other approaches have been proposed for the determination of m, but all have in common the approach of plotting some form of the applied load-deflection data to determine a slope or intercept.

It is not clear why so many researchers have adopted this approach without question. More importantly, there is absolutely no theoretical reason why equation (6) would hold. That is to say, there is no apparent physically based explanation as to why the slope of the log of indentation load versus the log of indentation diameter would be related, in any way, to the uniaxial tensile true-stress/true-strain hardening exponent. Any such limited agreement would only be fortuitous. In addition to the theoretical issues being raised, it is important to point out that even if there could have been some valid theoretical explanation for (6), it could never be used in practice to yield accurate results because of the high sensitivity of the power law. That is, very small variation in the Meyer coefficient, which ranges between 2 and 2.5 according to Tabor, would result in unacceptably large variations in YS, UTS, and in the power law flow curve (equation (4)).

I2S material model.

In view of the fact that there has been no defensible, sound, theoretical development over the past 100 years to relate hardness to YS or UTS, the approach taken by MPM is to use least-squares regression analysis to determine the best fit between YS or UTS, and hardness. Analyses have shown that the best correlation is linear with the following:

$$\begin{aligned} YS &= C_1\,(HBW) \\ UTS &= C_2\,(HBW) \end{aligned} \tag{7}$$

It has been demonstrated that the most accurate results are obtained if the regression data set is broken down into categories of strain-hardening potential. The constants in the above equation have been incorporated into the I2S software. All that is needed is for the user to run the test and the software will automatically report the Brinell hardness, YS, and UTs.

It is also possible to obtain a measure of ductility from the Brinell test. Tensile elongation is a measure of the ductility of a material. The engineering strain is defined as the average linear strain, and it is obtained by dividing the elongation of the gage length of the tensile specimen by its original gage length. If the uniform elongation is measured, it can be correlated with the Brinell strain. However, many test laboratories measure the total elongation after fracture, and this includes the necking strain. The total elongation can be correlated with the Brinell strain, but if specimens with different cross sections or gage lengths are used, there will be more scatter in the elongation than can be obtained using the uniform elongation. As discussed by Tabor, the Brinell strain can be defined as follows:

$$Brinell\ Strain\ (\%) = z\left(\frac{d}{D}\right) \tag{8}$$

where z is a constant, d is the indentation diameter, and D is the diameter of the indenter. This definition for Brinell strain follows that suggested by Tabor and others [7]. Additional

work will be needed in the future to relate the Brinell strain to conventional tensile ductility parameters.

Efficacy of the I2S tensile measurements.

The I2S load cell is calibrated annually using NIST traceable load cells. Similarly, the I2S displacement transducer is calibrated using NIST traceable displacement equipment on an annual basis. The I2S load cell is accurate to within 0.1% of range, which is comparable to conventional tensile test machine load cell accuracies. The displacement for Brinell indentation of steel is typically in the range of 0.001 inches to 0.050 inches. The I2S displacement transducer is accurate to within 0.02% of range. So, in terms of load and displacement measurement, the I2S accuracy is well within the precision of laboratory indentation testing equipment. The uncertainty has been quantified as will be discussed next.

Calibration and verification.

Brinell hardness calibration plates were purchased directly from NIST for verification of the calibration of the I2S for Brinell hardness determination. The average of the uncertainties reported by NIST for the calibration blocks tested in Figure 2 over a wide range of hard to soft materials is ± 2.7 HRB. The uncertainty in Brinell measurement of the 11 NIST calibration blocks is 1.06 %, and the ASTM E10 Brinell standard defines a permissible uncertainty of up to 3%. As shown in Figure 2, the I2S measurements are in very close agreement with the NIST certified values. Thus, it is clear that the uncertainty in determination of the YS or UTS comes mainly from the material model, so we now turn our attention to accuracy of the tensile data measured via the I2S.

In order to verify the I2S material model, conventional tensile specimens were machined from the NIST calibration block standards and tested in accordance with ASTM E 8. These measurements were made to determine the YS and UTS of the NIST calibration blocks. The data in Figure 3 compare the YS and UTS from the conventional tensile tests with the YS and UTS determined by the I2S. These data show that the I2S measured YS and UTS are within 10% (99% confidence interval) of the measured uniaxial tensile YS and UTS. In fact, the I2S measured YS and UTS match the conventional tensile data with a standard deviation of 3.3%. The low uncertainty is a reflection of the pristine microstructure of the NIST calibration blocks and would not be expected when testing production materials. It is expected that the I2S will deliver YS and UTS data within the data scatter range of the alloy being tested. It is recognized that various alloy systems have differing YS and UTS standard deviations. In the next section, the uncertainty associated with measuring tensile data for pipeline steels is investigated.

Comparison of I2S tensile data with benchmark data for line pipe steels.

Since the I2S has been developed for field measurement applications, I2S measurements and analyses have been performed for materials used in two line pipe benchmark studies. The first study was published in 2018 by the Pipeline Research Council International (PRCI) and the results are given in Reference [4]. In this study, over 50 line pipes were assembled and

these pipes consist of varying vintages, grades, manufacturers, seam types, and geometries. One objective of the PRCI was to provide a sample set representative of the total pipeline population in the US. These pipes were indented using the I2S and compared with conventional uniaxial tensile data provided by PRCI. The second study was published in 2021 by the Gas Technology Institute (GTI) [5]. In this work, a total of 70 pipes were assembled and, as was done by PRCI, conventional uniaxial tensile and hardness data were measured and reported. Since there is very little uncertainty in measuring Brinell hardness with the I2S, and since the I2S hardness data measured in the PRCI work was in very close agreement with laboratory hardness data, MPM used the GTI data to verify the I2S material model using the GTI laboratory hardness data as input. The benchmark results for each of these studies is discussed in turn below.

PRCI benchmark data.

MPM was not part of the original funded study since the PRCI was not aware of the MPM I2S technology at time the research program was established. Toward the end of the study, PRCI was notified concerning the I2S technology and kindly provided access to the 50 pipes so that the I2S measurements could be made. A total of 50 pipes were tested over a two day time period (9/19/2017 and 9/20/2017). Each pipe was surface ground over a ~4 inch x ~4 inch area to a smooth finish using an angle grinder, cleaned, and the I2S indentation test was performed up to 5 times for each pipe. An important advantage of the I2S methodology is that the surface grinding preparation requires only about 5 minutes per pipe. Shortly after MPM acquired the indentation data, the PRCI contracted with Bryan Lab to cut up the pipe sections and machine conventional mechanical behavior and hardness specimens for testing in accordance with applicable ASTM standards. The original PRCI data analysis done by MPM in 2017 was based on an early, generic, I2S material model. The PRCI data were re-evaluated by MPM in 2022 using the final I2S material model and the re-evaluation results are shown in Figure 4. As expected, the I2S Brinell hardness data are in close agreement with the Bryan Lab data (see Figure 2). The reason that the data scatter is larger than that shown in Figure 2 is because of variability of the piping material as compared with the metallurgically clean and refined NIST material. The I2S YS and UTS data also compare well with the Bryan Lab conventional ASTM E 8 tensile data (Figure 4).

The question remains as to how well the I2S measured YS and UTS data represent conventional uniaxial measurements. To address this question, statistical analyses were performed to quantify the accuracy of the I2S YS and UTS measurements. A useful measure of the variation in any data collection is the sample coefficient of variation:

$$\delta = \frac{S}{\bar{x}} \ , \qquad (9)$$

where, δ is the coefficient of variation, S is the sample standard deviation, and $\bar{x}$ is the sample mean. Simply stated, δ is the percentage of the mean attributable to one standard deviation. For the data in Figure 4, the measurements are symmetric about the unity slope line indicating that the Bryan Lab data and the I2S data have the same uncertainty for both YS and UTS. The coefficients of variation for the 50 pipes of the PRCI is:

$$\delta(\text{YS}) = 5.7\%$$
$$\delta(\text{UTS}) = 6.7\%$$

It is, of course, recognized that the coefficient of variation depends on the alloy system being analyzed. However, Wirsching has reported typical coefficient values for metals, and these

are shown in Table 1. Thus, we conclude that the data scatter for the 50 PRCI pipes is consistent with the data in Table 1, and the standard deviation for the uncertainty is the same whether the YS or UTS is measure by the conventional ASTM E8 specimens or by the I2S indentation method.

GTI benchmark data.

GTI conducted tests on over 70 gas transmission line pipes. The non-destructive tests on the GTI pipes were performed by two organizations (Frontics and MMT), after which GTI cut the pipes and performed conventional mechanical property tests including hardness and tensile. GTI was not aware of the MPM development of the I2S technology, so MPM was not part of the GTI site testing. However, for the purpose of benchmarking the I2S material model, indentation measurements on the pipes are not necessary as MPM has demonstrated that the Brinell hardness measurements have very low uncertainty and accurately reflect the Brinell hardness of the material. What is of interest with the GTI data is benchmarking of the I2S material model. So, GTI kindly provided the Reference [5] report and the GTI hardness data were used in the I2S material model to determine YS and UTS. The results are shown in Figure 5. With the exception of two outliers, the data in Figure 5 show that the measurements are symmetric about the unity slope line indicating that the conventional tensile data and the I2S data have the same uncertainty for both YS and UTS. The coefficients of variation for the 70 pipes of the GTI study are:

$$\delta(\text{YS}) = 6.0\%$$
$$\delta(\text{UTS}) = 5.7\%$$

As in the PRCI study, we conclude that the data scatter for the 70 GTI pipes is consistent with the data in Table 1. The standard deviation for the uncertainty is the about the same whether the YS or UTS is measured by the conventional ASTM E8 specimens or by the I2S indentation method. This is essentially the same conclusion as obtained with the PRCI study.

There were several findings regarding the surface indentation methods of the two organizations that participated in the GTI study (Frontics and MMT) reported in Reference [5] that are worth mentioning. The MMT method is a low force scratch test that was originally developed to perform hardness scans on non-planar surfaces such as pipe elbows. The MMT data in Figure 6 show that the light applied force is not applicable for mechanical property determination of many pipe material microstructures. While seamless pipe is normalized and annealed, thereby producing a very homogenous microstructure across its thickness, welded pipe is produced from hot rolled plate, or strip, that usually exhibits through-thickness property variations. In these materials, differences in grain size, or in the pearlite interlamellar distance, are produced. These heterogeneities are produced by localized through-thickness differences in temperature as the plate is rolled, and then subsequently cooled. In addition, forming and welding procedures often produce significant residual stresses and cold work. The near surface cold work tends to make the outer layers of the pipe stronger, thereby requiring a deeper probing of the material for accurate YS determination. As a result of the MMT data in Figure 6, GTI concluded,

> "The observed trends likely indicate that the MMT HSD "surface scratch-type" technique interrogates mostly the outer layers of the pipe wall while the Frontics AIS "indentation-type" technique may in effect test deeper into the pipe wall."

The Frontics and I2S methods both test much deeper into the pipe wall than the MMT method, and thereby obtain the bulk tensile properties.

While the indentation methods of Frontics and I2S are similar, the material models are very different. Figure 7 shows the GTI study results obtained by Frontics. Unlike MMT, the data are located on the unity slope line, but the data scatter is much larger than the data obtained with the I2S (Figure 5). This is largely due to the fact that the Frontics material model uses a power law fit to the data. The lack of a physical basis for this assumption was discussed earlier in relation to equation (4). Reference [8] reports the following for the Frontics methodology:

Step 0 Determination of **contact area**

$a \rightarrow a_c$

Step 1 Derivation of **stress-strain points**

$$\sigma = \frac{L}{\pi a^2}\frac{1}{\psi}, \quad \varepsilon = \frac{\alpha}{\sqrt{1-(a/R)^2}}\frac{a}{R} = \alpha \tan\gamma$$

Step 2 Determination of **flow curve**

$\sigma = K\varepsilon^n$ for Hollomon-type materials

$\sigma = A + E_r\varepsilon$ for FCC materials

Step 3 Determination of **yield strength** (3-1) and **tensile strength** (3-2)

$\sigma_y = K(\varepsilon_y + b)^n$ yield strength

$\sigma_{UTS} = Kn^n$ tensile strength

(Reference [8])

The reasons for the added data scatter are apparent. Most materials are not well represented by a simple power law. Even if they were, determination of the power law constants will introduce uncertainty. After the power law is determined, the yield stress is calculated by the intersection of the elastic modulus and the plastic flow curve. This adds more uncertainty.

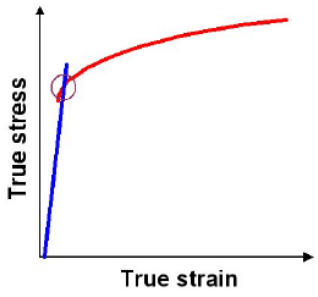

$K\varepsilon_y^n = E(\varepsilon_y - 0.002)$ ➔ ε_y determination

$\sigma_y = K(\varepsilon_y + b)^n$

(Reference [8])

So, the data scatter for the Frontics method, as shown in Figure 7, is not due to the method of indentation as with the MMT technology. Rather, it is due to the use of a non-physically based material model that is cumbersome and introduces unnecessary uncertainty.

Fracture toughness from Charpy specimens.

In cases where a pipe or other in-service structure is found to have failed the hardness and tensile screening using the I2S, further analyses will likely be required. In most cases, the plane strain fracture toughness (K_{IC} and J_{IC}) will be need for comparison with the finite element determined applied J-integral. The question addressed here is how to obtain J_{IC} from in-service line pipe measurements. Some have suggested using the Sailors-Corten correlation found in API 579, Appendix F.4.5:

$$K_{IC} = 15.5(CVN)^{0.5} \quad (10)$$

where CVN refers to Charpy absorbed energy.

MPM is strongly opposed to any correlation between Charpy energy and fracture toughness because these correlations have been shown, time and again, to only work for a limited alloy condition. When applied to other materials, the results are not correct and are not conservative. The original work to obtain equation (10) is reported in Reference [9]. The data base used for the equation development included both irradiated and unirradiated pressure vessel steels (A533B, A517F, A302B, ABS-C, and A542). Candidate equations were partitioned into three categories: lower shelf, transition, and upper shelf. Equation (10) was selected over the Rolfe-Barsom equation and was considered to be the best fit to unirradiated data for four plate materials: A533B, A517F, and A542). The basis for rejecting the Rolfe-Barsom equation was that it simply did not fit the pressure vessel data set since it was based heavily on rotor steels. Equation (10) was separated from other fitted equations in that study and put into the category of "*Low Temperature and Transition Range*" equations. It is reported in Reference [9] that when all of the data were plotted and fit "the slope of the line did not produce a good fit for most of the data". As a result, they developed guidelines to eliminate materials and data sets so that "major attention was focused on pressure vessel steels similar to A533B steel". So, to eliminate transition region data scatter, "attention was focused upon the lower bound of the Charpy energy band". All impact data of Reference [9] with Charpy energy less than 5 ft-lbs was eliminated. All impact data on the upper shelf was eliminated by setting an arbitrary cut off at 50 ft-lbs. As a result of poor least squares regression on the culled down data set, further data were eliminated: "These considerations led to a conscious attempt to select only data where metallurgical structure was most uniform (from T/4 to 3T/4) and typical of thick pressure vessel steel". So, by their own work Sailors and Corten defined Equation (10) as applicable to only a very limited data set.

So, in summary, equation (10) was developed for a very specific material set, and during the development Sailors and Corten showed that the equation is not of general applicability since they had to eliminate materials and metallurgical conditions from the data base to get an acceptable fit. In other words, the very source document for equation (10) clearly states that this equation will not work at all for other materials.

Miniaturized fracture toughness testing.

Since impact energy correlations cannot ever ensure reasonable, yet conservative, fracture toughness data, MPM's approach is to cut small amounts of material from the pipe and perform instrumented impact tests in accordance with either ASTM E23 (CVN) or ASTM E2248 (MCVN), and E2298. A photograph of the E2248 miniaturized Charpy V-notch (MCVN) is shown in Figure 8 on a line pipe to show the size scale of the specimen. Since CVN and MCVN specimens yield the same fracture toughness data, either specimen can be used depending on pipe wall thickness needs. MPM has applied its mechanics model to enable determination of the J-resistance (J-R) curve and J_{IC}. Example data are shown in Figures 9 and 10 for a ferritic steel. The specimen in Figure 9 is a stress field modified specimen with side constraint modifications which have been shown to produce the same constraint in the MCVN as in a conventional CVN (Reference [10]). In cases where highly ductile materials need to be tested, MPM has developed a side-arm constraint test for the line pipe industry that can be machined from the pipe wall (Reference [11]) and impact tested on a standard Charpy machine. Many tests have been conducted over the past decade to verify the efficacy of the CVN and MCVN fracture mechanics model used to analyze load-deflection data obtained from notched Charpy specimens to determine plane-strain fracture toughness. Two examples are presented here. Data from conventional ASTM E1820 test specimens were compared with the results from instrumented Charpy specimens.

Comparison of conventional ASTM E 1820 and Charpy fracture toughness data for a structural steel plate.

Seven static fracture toughness tests were performed on specimens machined from a structural carbon steel block. The testing was performed in accordance with the procedures given in ASTM E 1820 for 0.5 inch thick single edge bend (SEB) specimens. The test specimens were machined, EDM chevron-notched, and tested at -10° F in accordance with the requirements given in Annex A of ASTM E 1820. Precracking was performed in accordance with the standard to a nominal a/W depth of 0.5 inches. The tests were conducted using the MPM AC Potential Drop (ACPD) crack length measurement system. A summary of the key fracture toughness test results is given in Table 2.

Three side-grooved Charpy V-Notch (CVN) instrumented impact tests were performed on specimens machined from the same structural steel block as for the conventional fracture toughness specimens. Impact testing was in accordance with the testing procedures given in ASTM E 23 and E 2298. A summary of key instrumented Charpy test results is given in the Table 3. The instrumented data were analyzed to determine fracture toughness using 1[the fracture toughness mechanics model described in [11]. The average fracture toughness for the conventional test method is 96.5 ksi$\sqrt{in}$, as compared with 87.1 ksi$\sqrt{in}$ for the instrumented Charpy specimens. The close agreement in the measured fracture toughness for the two methods demonstrates that the CVN specimen mechanics model is capable of predicting valid fracture toughness results without the need for fatigue pre-cracking and laborious post-test measurements.

Comparison of conventional ASTM E 1820 and Charpy fracture toughness data for a welded steel plate.

Three 0.5T SE(B) CTOD specimens were machined from welded plates and tested in accordance with ASTM E 1820 requirements. In addition, three CVN specimens were machined and tested in accordance with ASTM E 23 and E2298 requirements. The static fracture toughness test specimens were EDM chevron notched, fatigue pre-cracked, and tested at 40° F. Ductile crack initiation and extension were determined from the unloading compliance data. The data were analyzed to determine CTOD and fracture toughness. A nominal a/W depth of 0.5 was successfully attained during precracking. As indicated in Table 4, the final crack size straightness requirements could not be met for all of the specimens. This is due to the parabolic shape of the final crack. The data were analyzed to determine whether all of the CTOD and J-R measurement requirements were met, and the results are summarized in Table 4. Specimen FP2-1 was tested past the capacity for the crack mouth opening gage resulting in a final crack extension that does not represent the last unloading compliance measurement. In addition, FP2-2 did not meet the crack extension prediction comparison. Specimen FP2-3 however, did meet the crack extension prediction comparison. Although it was not possible to satisfy all of the E 1820 requirements, most of the validity requirements were met. The J_{IC} measurements range from 1,736 to 2,918 in-lb/in^2, and the CTOD δ_{IC} measurements range from 0.117 to 0.193 inches as shown in Table 4.

A summary of key instrumented Charpy test results is given in the Table 5. The instrumented data were analyzed to determine fracture toughness as previously discussed. As shown in Table 5, the J_{IDN} measurements range from 618 to 2,315 in-lb/in^2. For specimen P2-3, the J_{IDN} is above the maximum J-integral capacity for the specimen. The J_{IDN} range compares well with the conventional 0.5 T single edge bend specimen data. As is typical, there is considerable scatter in fracture toughness data and the CVN determined fracture toughness is usually on the conservative lower range of the E 1820 data.

Summary and Conclusions.

Technologies are now available to fully respond to the requirements of the Mega Rule and to interrogate other in-service structures and components. These technologies offer a means for substantial improvement of safety to the public. The I2S is a physically based method for non-destructive measurement of YS and UTS. Unlike the "surface scratch" method, it probes deeply into the component to accurately determine the bulk material properties. In cases where the tensile properties do not meet specifications, the MPM miniature specimen fracture toughness technology will provide the needed data for a structural analysis.

References

[1] I. M. Hutchings, "The contributions of David Tabor to the science of indentation hardness," J. Mater. Res., Vol. 24, No. 3, March 2009.
[2] D. Tabor: The hardness and strength of metals. J. Inst. Metals 79, 1 (1951).
[3] D. Tabor: A simple theory of static and dynamic hardness. Proc. R. Soc. London, Ser. A 192, 247 (1948).

[4] B. Amend, S. Riccardella, A. Dinovitzer, "PRCI NDE 4-8 – Material Verification – Validation of In Situ Methods for Material Property Determination," Pipeline Research Council International (PRCI) NDE 4-8 PR-335-173816, May 8, 2018.

[5] M. Manning, "Validating Non-Destructive Tools for Surface to Bulk Correlations of Yield Strength, Toughness, and Chemistry," GTI Project No. 22428/22429; DOT/PHMSA Contract No. 693, September 28, 2021.

[6] Statistical Variation in Material Properties, Wordpress, (2023, December 11), p. 803, https://cmmpackpr.files.wordpress.com/2010/12/d02_stat_02_statistical_variations_in_material_properties.pdf.

[7] MILHDBK. 1994. *Military Handbook: Metallic Materials and Elements for Aerospace Vehicle Structures,* MIL-HDBK-5G, 2 Vols., U.S. Dept. of Defense, MIL-HDBK-5 Coordination Activity. Wright-Patterson AFB, OH.

[8] "Measurement of Yield strength, Tensile strength and Fracture toughness of API 5L pipe using Instrumented Indentation Testing", Frontics report to GTI, June, 2019.

[9] H. T. Corten, R. H. Sailors, "Relationship Between Material Fracture Toughness Using Fracture Mechanics and Transition Temperature Tests", August 1, 1971.

[10] Manahan, Sr., M.P., "Miniaturized Charpy Test for Reactor Pressure Vessel Embrittlement Characterization", Effects of Radiation on Materials: 18th International Symposium, ASTM STP 1325, R.K. Nanstad, M.L. Hamilton, F.A. Garner, and A.S. Kumar, Eds., American Society for Testing and Materials, 1997.

[11] Manahan, Sr., M. P., "Constraint-modified Charpy-Sized Fracture Toughness Specimen for Line Pipe Testing", Feature Article AIST, October, 2013.

Table 1. Typical coefficients of variation for various mechanical property tests.

Variable	Typical δ %
Yield strength of metals	7
Ultimate strength of metals	5
Modulus of elasticity of metals	5
Fracture toughness of metals	15
Tensile strength of welds	10
Compressive strength of concrete	15
Strength of wood	15
Cycles to failure in fatigue	50
Crack growth rate in fatigue	50
Strength for a given life in fatigue	10

Source: Reference [6], p. 803; Reference [7].

Table 2. Fracture toughness data for ASTM E1820 0.5 T SEB specimens tested at -10 F.

Specimen ID	Precrack Length a_o	Uncracked Ligament b_o	J_{Qc}	K_{JQc}	J_{Qc} Qualified as J_{Ic} [a.]	Crack Variance Verification[b.]
	(in)	(in)	(in-lb/in^2)	(ksiVin)		
SEB -1	0.5327	0.4673	217.4	83.2	Yes	Pass
SEB -2	0.5216	0.4784	295.3	96.8	Yes	Fail [d.]
SEB -3	0.5248	0.4752	400.4	113.3	No [c.]	Pass
SEB -4	0.5302	0.4698	200.9	80.1	Yes	Pass
SEB -5	0.5202	0.4798	174.4	74.5	Yes	Pass
SEB -6	0.5159	0.4841	254.8	90.2	Yes	Pass
SEB -7	0.5119	0.4881	595.5	138.1	No [e.]	Pass

Note:

a. Per ASTM E 1820, Annex A6, in the case of fracture instability before stable tearing, J_{Qc} may be qualified as J_{Ic} if it meets the following two conditions:
   1. B, $b_o \geq 100\ J_{Qc}/\sigma_Y$
   2. $\Delta a_p < 0.2$ mm + $J_{Qc}/2\ \sigma_Y$

b. Per ASTM E 1820, none of the nine physical measurements of initial crack size shall differ by more than 0.05B from the average a_o.

c. Specimen 4-3 did not meet condition 1 specified above, as b_o (0.4752 in) is not greater than $100*J_{Qc}/\sigma_Y$ (0.4883 in). However, it is close.

d. For Specimen 4-2, one out of the nine crack length measurements differed from the average by 0.028 inches. This exceeds the tolerance of 0.025 inches by 0.003 inches.

e. Specimen 4-7 did not meet condition 1 specified above, as b_o (0.4881 in) is not greater than $100*J_{Qc}/\sigma_Y$ (0.7257 in).

Table 3. Fracture toughness data obtained from instrumented striker tests on CVN plate specimens tested at -10 F.

ID	Optical Encoder Impact Energy (ft-lb)	Instrumented Impact Energy (ft-lb)	Energy at General Yield Load[b] (ft-lb)	Energy at Peak Load (ft-lb)	Peak Load (lbf)	J_{idn} [a] ($in\text{-}lb/in^2$)	K_{idn} [a] ($ksi\sqrt{in}$)
CVN -1	11.06	10.51	2.40	9.47	4169.4	152.6	70.0
CVN -2	4.61	3.66	-	1.82	3407.0	253.5	89.6
CVN -3	5.72	4.82	-	4.21	3877.3	325.4	102.1

Note:
[a] The fracture toughness values reported are for notched and side-grooved CVN specimens. The final fracture toughness values are reported with the subscript "Idn" to indicate Mode I loading, dynamic testing, and a notch was used to initiate the crack.

Table 4. Fracture toughness data for ASTM E1820 0.5 T SEB weld specimens at 40 F.

ID	Precrack Length from Calculation a_{0q} (in)	Uncracked Ligament from Calculation b_0 (in)	Crack Extension Prediction (in)	Crack Extension Check [a]	δ_{IC} (in)	Qualified as δ_{IC} [b]	J_{IC} ($in\text{-}lb/in^2$)	Qualified as J_{IC} [c]	K_{JIC} ($ksi\sqrt{in}$)
FP2-1	0.531	0.463	0.092[d]	Fail	0.0117	Yes	1736.1	Yes	233.7
FP2-2	0.492	0.505	0.075	Fail	0.0193	Yes	2918.0	Yes	303.0
FP2-3	0.517	0.484	0.085	Pass	0.0177	Yes	2634.7	Yes	287.9

Note:
a. Per ASTM E 1820, the crack extension predicted from elastic compliance at the last unloading shall be compared with the measured physical crack extension Δap. The difference between these shall not exceed $0.15\Delta ap$ for crack extensions less than 0.2 b_0, and the difference shall not exceed 0.03 b_0 afterward.
b. Per ASTM E 1820, Annex A11, δ_Q may be qualified as δ_{Ic} if it meets the following condition:
$b_o \geq 10m\delta_Q$
c. Per ASTM E 1820, Annex A9, J_Q may be qualified as J_{Ic} if it meets the following two conditions:
$B \geq 10\ J_Q/\sigma_Y$
$b_o \geq 10\ J_Q/\sigma_Y$
d. The crack mouth opening was extended past the measurement limit of the crack mouth opening gage. Crack extension was calculated to the greatest crack mouth opening measured.

Table 5. Fracture toughness data obtained from instrumented striker tests on CVN weld specimens tested at 40 F.

ID	Optical Encoder Impact Energy (ft-lb)	Instrumented Impact Energy (ft-lb)	Energy at General Yield Load (ft-lb)	Energy at Peak Load (ft-lb)	Peak Load (lbf)	J_{IDN} [a] ($in\text{-}lb/in^2$)	K_{IDN} [a] ($ksi\sqrt{in}$)
P2-1	36.51	34.75	1.70	8.49	3037.5	617.8	140.3
P2-2	44.89	44.83	1.87	25.01	3679.5	1798.5	239.4
P2-3	55.15	54.27	1.73	30.61	3690.1	2315.3 [b]	271.6

Note:
[a] The fracture toughness values reported are for notched CVN specimens. The fracture toughness values are reported with the subscript "IDN" to indicate Mode I loading, dynamic testing, and a notch was used to initiate the crack.
[b] The J_{IDN} value for P2-3 is above the maximum J-integral capacity for the specimen (2213 $in\text{-}lb/in^2$). The J- R curve is defined as the data in a region bounded by the coordinate axes and the J_{max} and a_{max} limits.

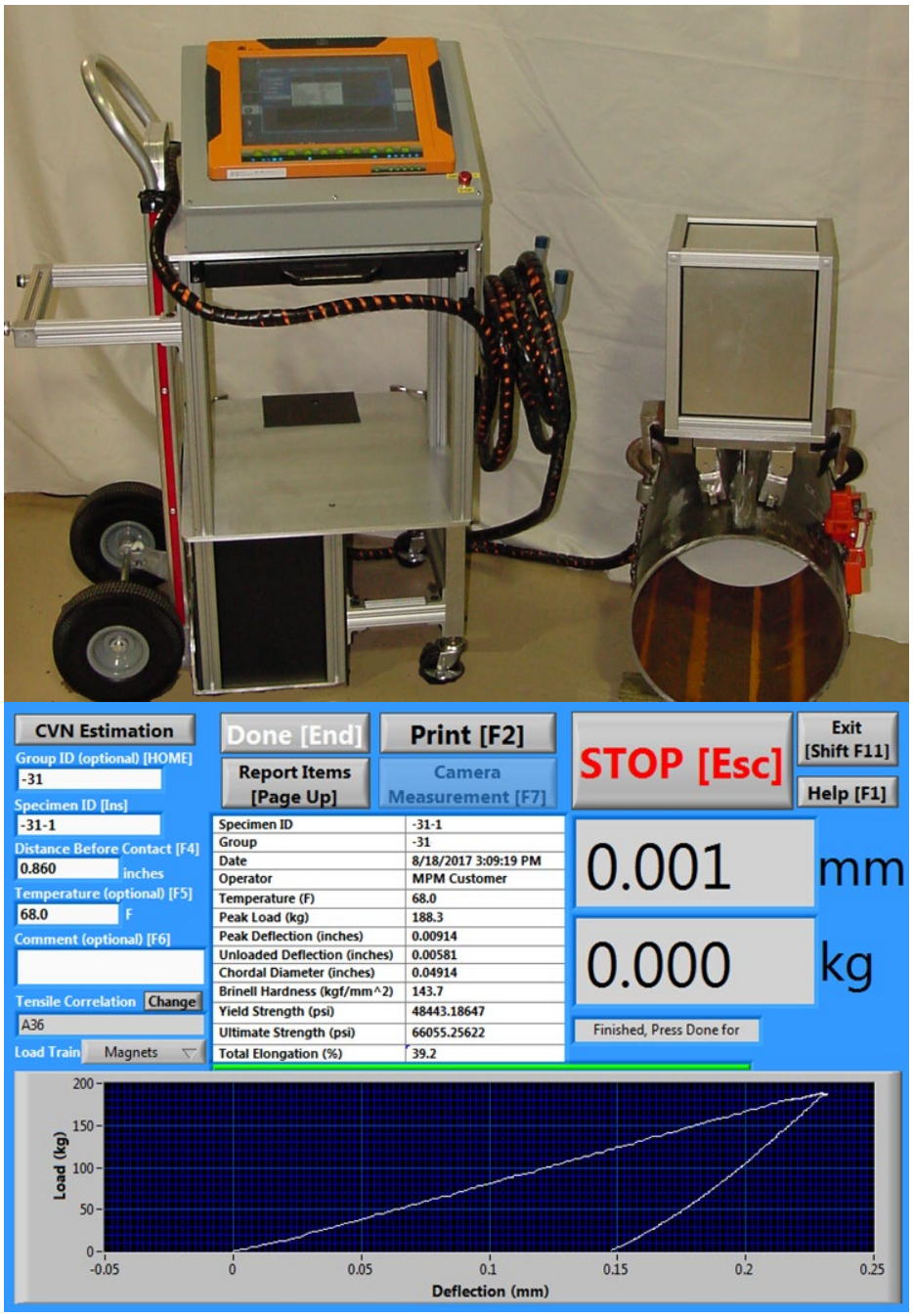

Figure 1. (top) MPM I2S installed on a 16 inch diameter pipe in preparation for an indentation test. (bottom) Example I2S indentation data.

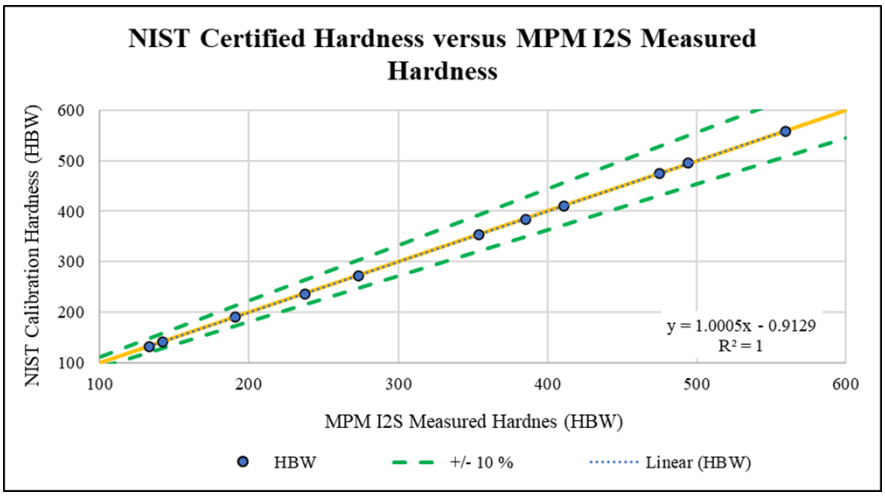

Figure 2. Comparison of I2S measured Brinell hardness with NIST certified values for eleven NIST calibration blocks covering the range of 125 HRB to 560 HRB. As indicated by the R^2=1 value, the I2S measurements are in very close agreement with the NIST certified values.

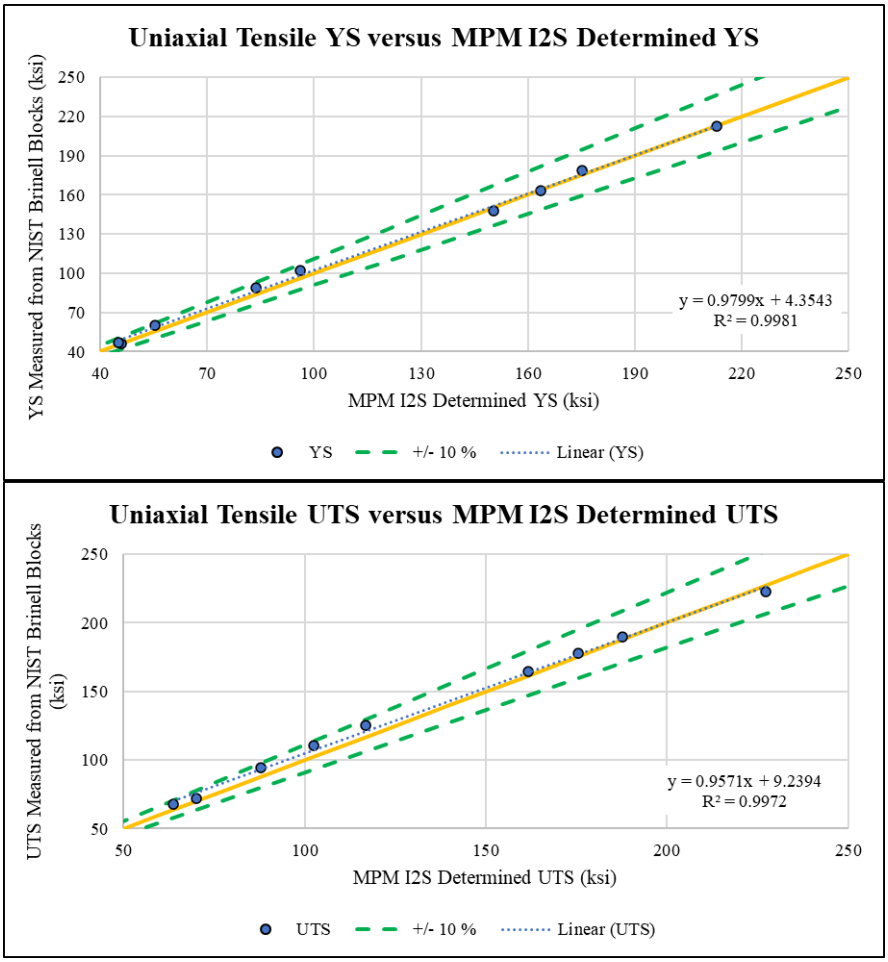

Figure 3. I2S measured YS and UTS compared with tensile data from conventional test specimens that were machined from the NIST calibration blocks.

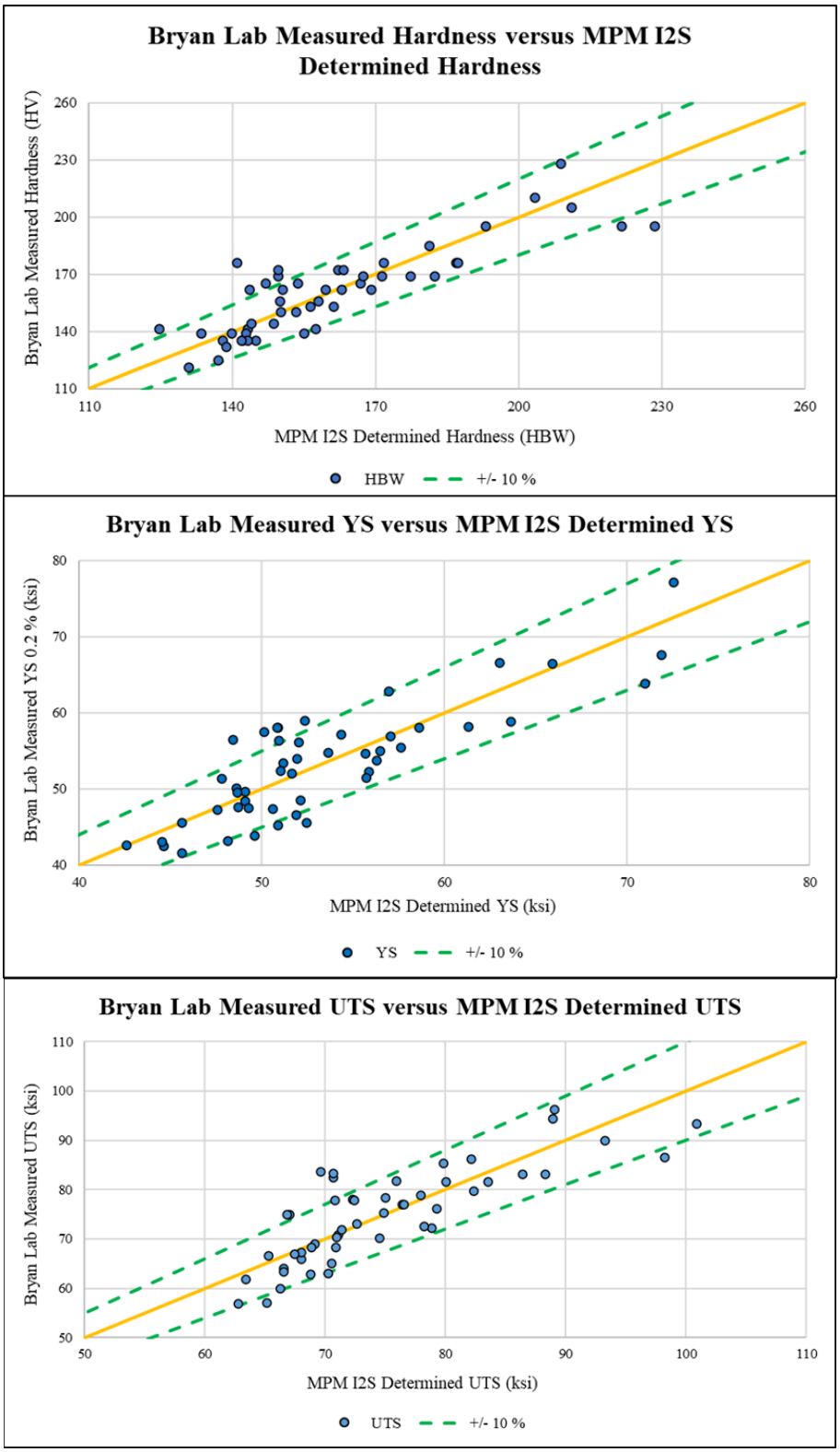

Figure 4. I2S data are compared with the PRCI conventional specimen hardness, YS, and UTS data. The I2S YS and UTS data match the conventional tensile data with standard deviations of 5.7% and 6.7%, respectively.

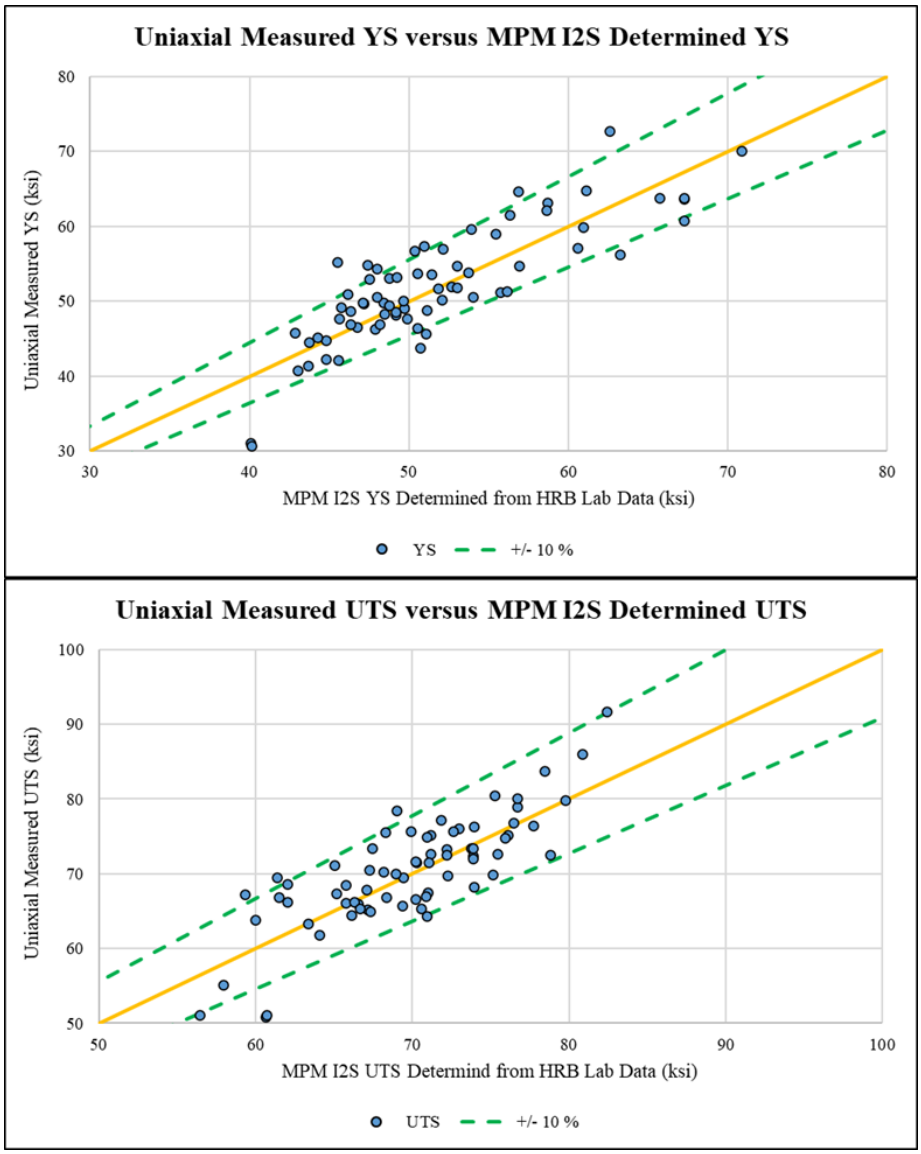

Figure 5. I2S data are compared with the GTI conventional specimen YS and UTS data. With the exception of two outliers, the I2S YS and UTS data match the conventional tensile data with standard deviations of 6.0% and 5.7%, respectively.

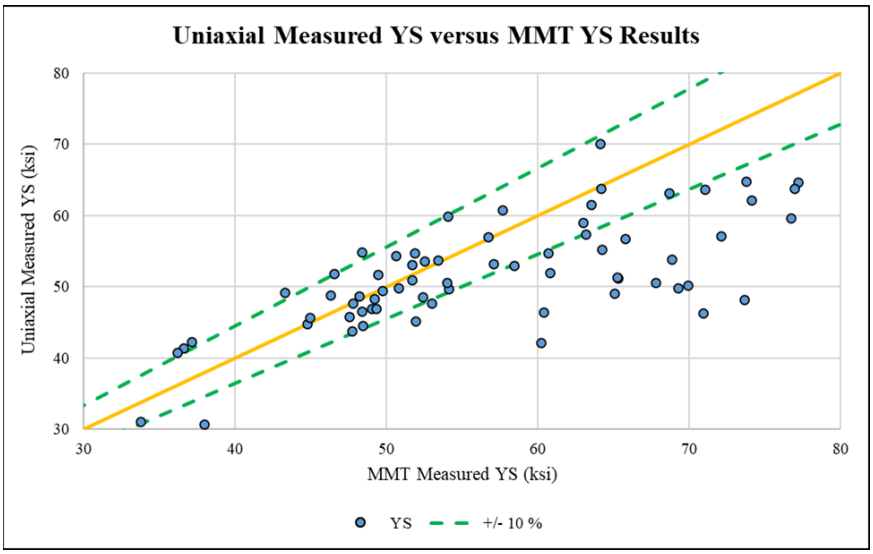

Figure 6. MMT data are compared with the GTI conventional ASTM E8 specimen YS data. These results can be compared with the I2S upper plot in Figure 5 which shows the correct bulk material results as measured by the I2S. Since the MMT technique only interrogates the outer layers of the pipe, the MMT measurements are not accurate for pipes with surface hardnesses that differs from the bulk material hardness and strength.

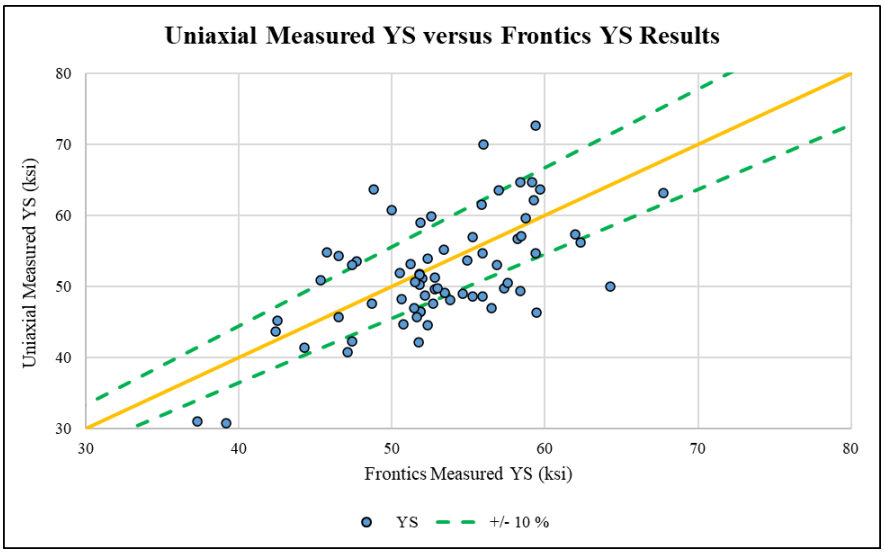

Figure 7. Frontics data are compared with the GTI conventional ASTM E8 specimen YS data. Although the data are on the unity slope line, the data scatter is much larger than the data obtained with the I2S (see Figure 5).

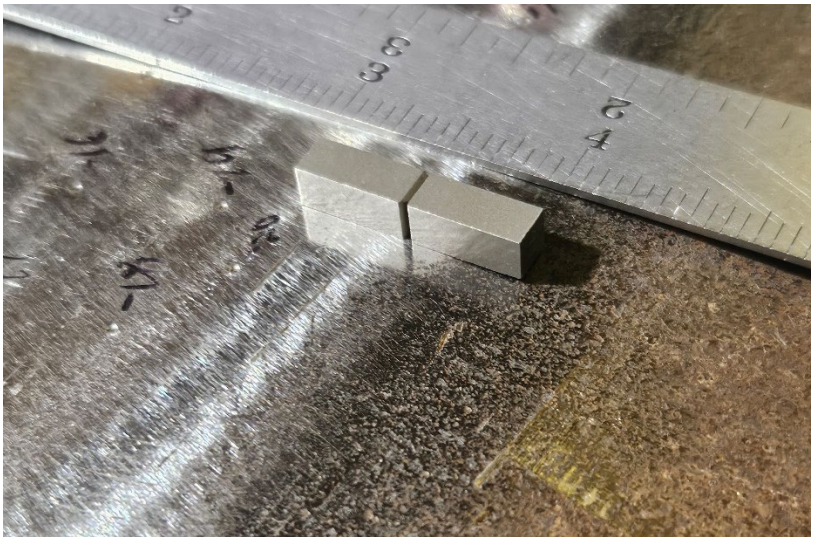

Figure 8. MCVN specimen on a line pipe next to a surface ground area where I2S indentations have been made. The material for the MCVN specimen can be trepanned from the pipe surface and weld repaired.

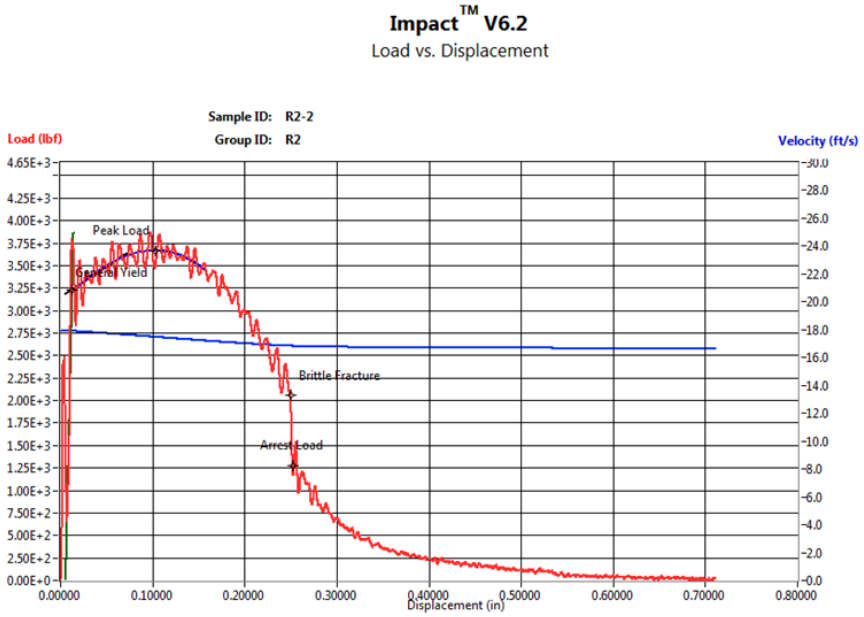

	Load (lbf)	Displacement (in)	Velocity (ft/s)	Time (s)	Energy (ft lbf)
General Yield	3.2346E+3	1.287E-2	1.789E+1	5.981E-5	1.84814E+0
Peak Load	3.6648E+3	1.024E-1	1.747E+1	4.819E-4	2.80830E+1
Brittle Fracture	2.0637E+3	2.497E-1	1.682E+1	1.199E-3	6.66639E+1
Arrest Load	1.2734E+3	2.522E-1	1.681E+1	1.211E-3	6.70074E+1
End of Signal	1.4648E+1	7.100E-1	1.665E+1	3.497E-3	7.63517E+1

Figure 9. Example instrumented striker data showing general yield load (yielding across the uncracked ligament), peak load (beginning of stable crack propagation), brittle fracture load (unstable crack pop), and arrest load (arrest of the unstable crack).

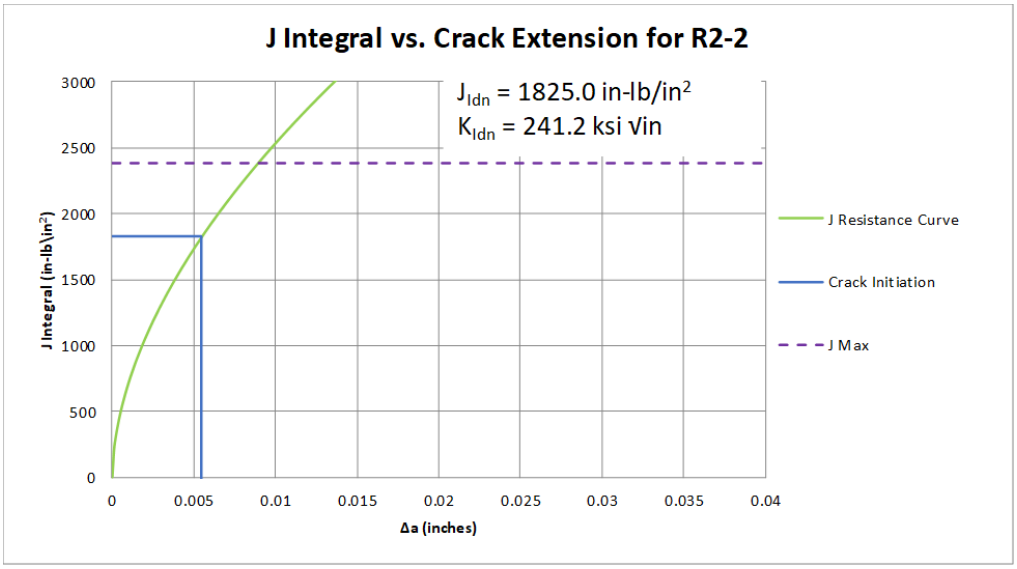

Figure 10. J-R curve and a conservative, yet accurate J_{IC} determination from the instrumented striker data of Figure 9. The subscript "IDN" defines the test as a Mode I, dynamic, test with a crack starter notch.